British Journal of Pharmacology (2002) 136, 201–206

www.nature.com/bjp

Modification of NMDA responses by tri-*n*-butyltin in rat brain neurons

[1]Yumiko Kanemoto, [1]Hitoshi Ishibashi, [1]Shinichiro Matsuo, [2]Yasuo Oyama & *,[1]Norio Akaike

[1]Cellular and System Physiology, Graduate School of Medical Sciences, Kyushu University, Fukuoka 812-8582, Japan and [2]Laboratory of Cellular Signaling, Faculty of Integrated Arts and Sciences, The University of Tokushima, Tokushima 770-8502, Japan

1 The effects of the organotin, tri-*n*-butyltin (TBT), on *N*-methyl-D-aspartate (NMDA) induced membrane currents were investigated in order to evaluate possible neuronal actions of this toxic environmental pollutant. Experiments were conducted on neurons acutely dissociated from the rat dorsal motor nucleus of vagus (DMV) using the nystatin-perforated patch clamp recording technique.

2 In Mg^{2+}-free physiological recording solutions, the application of NMDA to single DMV neurons held at a holding potential (V_H) of −40 mV evoked an inward current which rapidly reached a peak before declining to a steady-state inward current. This was followed, immediately after NMDA washout, by a transient outward current. TBT (100 nM) reversibly caused a slight reduction in the inward currents and greatly increased the amplitude of the outward currents.

3 The reversal potential of the NMDA-induced outward current in the presence of TBT was −86.7 mV, close to the theoretical K^+ equilibrium potential of −85.7 mV.

4 The NMDA-induced outward current was completely blocked when the K^+ in the internal solution was replaced with equimolar Cs^+. Under these conditions, the NMDA induced current was more sustained and was unaffected by TBT.

5 The NMDA-induced outward current was markedly inhibited by 5 mM tetraethylammonium chloride and 300 nM charybdotoxin, and it was abolished by removal of extracellular Ca^{2+}, suggesting that the outward current was due to the activation of Ca^{2+}-activated K^+ channels by Ca^{2+} influx through NMDA receptors.

6 In conclusion, in rat DMV neurons, TBT potentiates the Ca^{2+}-activated K^+ current induced by NMDA application without having any direct effects on the NMDA-induced inward current. Given the significant role of NMDA receptor mediated excitation in various physiological and pathological processes, the modulation of this response by TBT may have an important influence on neuronal function.

British Journal of Pharmacology (2002) **136,** 201–206

Keywords: Tri-*n*-butyltin; dorsal motor nucleus of vagus; *N*-methyl-D-aspartate; Ca^{2+}-activated K^+ current; nystatin-perforated patch recording

Abbreviations: $[Ca^{2+}]_i$, intracellular concentration of Ca^{2+}; DMV, dorsal motor nucleus of vagus; EC_{50}, half-maximum effective concentration; I_{KCa}, Ca^{2+}-activated K^+ currents; *N*-methyl-D-aspartate (NMDA); TBT, tri-*n*-butyltin; V_H, holding potential

Introduction

Organotins, like tri-*n*-butyltin (TBT), have been widely used in a variety of consumer and industrial products including agricultural pesticides, antifouling paints for ship hulls and stabilizers for polyvinyl-chloride plastics (Luijten, 1971; Ohhira *et al*., 1999). Despite the use of TBT being prohibited in Japan since 1990, marine pollution by this highly toxic contaminant has continued (Yamamoto, 1994; Harino *et al*., 2000). As TBT accumulates in edible mollusks and fishes (Shim *et al*., 1998; Harino *et al*., 2000), it represents a potential danger for human health.

The immunotoxic actions of TBT have been well documented and the underlying mechanisms intensively investigated (Snoeij *et al*., 1987; Ghoneum *et al*., 1990; Raffray & Cohen, 1993; Whalen *et al*., 1999). TBT is also toxic to the developing rat nervous system (O'Callaghan & Miller, 1988; Ema *et al*., 1991a, b) and in dissociated rat cerebellar neurons, at nanomolar concentrations, increases intracellular Ca^{2+} ($[Ca^{2+}]_i$) by both increasing membrane Ca^{2+} permeability and releasing Ca^{2+} from intracellular stores (Oyama *et al*., 1993; Ueha *et al*., 1996). An increase in $[Ca^{2+}]_i$ affects a wide range of cellular proteins, including the functions of various receptor-ionophore complexes (Inoue *et al*., 1986; Balasubramanian *et al*., 1996; De-Koninck & Mody, 1996; Kyrozis *et al*., 1996). Therefore, we investigated the effect of TBT on the membrane currents induced by *N*-methyl-D-aspartate (NMDA) in acutely dissociated rat dorsal motor neurons using nystatin-perforated patch recordings (Horn & Marty, 1988; Akaike & Harata, 1994).

*Author for correspondence;
E-mail: akaike@physiol2.med.kyushu-u.ac.jp

Methods

Preparation

Neurons were dissociated from the dorsal motor nucleus of the vagus nerve (DMV) of rats, as described previously (Doi *et al*., 1999). Briefly, 10–16-day old Wistar rats (Japan Charles River Laboratory, Shizuoka, Japan) were decapitated under pentobarbital sodium anaesthesia under the 'Guiding Principles for the Care and Use of Laboratory Animals' approved by the Japanese Pharmacological Society. The brain was quickly removed from the skull and then sliced at a thickness of 400 μm with a microslicer (DTK-1000, Dosaka, Osaka, Japan). The slices were preincubated in the well-oxygenated standard external solution containing 0.1 mg ml^{-1} pronase (Sigma Chemical Co.) for 40 min at 31°C, followed by the standard external solution containing 0.1 mg ml^{-1} thermolysin (Calbiochem-Novabiochem Co., Darmstadt, Germany) for 20 min at 31°C. Thereafter, the DMV region was micropunched out from the slice, transferred to a culture dish (Primaria 3801, Becton Dickinson, NJ, U.S.A.) and individual neurons were dissociated mechanically with a fire-polished Pasteur pipette. The dissociated DMV neurons subsequently adhered to the bottom of the dish within 20 min.

Electrical measurements and data analysis

Single DMV neurons were voltage-clamped using the nystatin-perforated patch recording mode as described previously (Horn & Marty, 1988; Akaike & Harata, 1994). Patch electrodes were fabricated from glass capillaries (G-1.5, Narishige, Tokyo, Japan) using a vertical puller. The standard patch pipette (internal) solution contained (in mM) K-methanesulphonate 70, KCl 80, HEPES 10. The pH was adjusted to 7.2 with Tris base. In some experiments, K-methanesulphonate and KCl were replaced with 70 mM Cs-methanesulphonate and 80 mM CsCl. Nystatin (Sigma) was first dissolved in methanol (10 mg ml^{-1}) before being added to the pipette solution at a final concentration of 200 μg ml^{-1} just before use. The resistance between the patch pipette filled with the internal solution and reference electrode in the standard solution was 5–8 MΩ.

Dissociated neurons were visualized with a phase-contrast inverted microscope (Diaphot-TMD, Nikon, Tokyo, Japan). Currents were recorded, and voltage controlled, using a patch clamp amplifier (CEZ-2300, Nihon-Kohden, Tokyo, Japan). After stable patch perforation, the series resistance ranged from 10 to 25 MΩ, and was compensated in the same manner as previously described (Doi *et al*., 1999). Membrane currents were monitored on both a storage oscilloscope (Textronix 5111A, Sony, Tokyo, Japan) and a pen recorder (Recti-Horiz 8K, Nippondenki San-Ei, Tokyo, Japan). Both membrane potential and current signals were stored using a digital audio tape recorder (RD-130TE, TEAC, Tokyo, Japan). Membrane currents were filtered at 1 kHz, digitized at 4 kHz, and stored on a computer using pCLAMP software (Axon Instruments Inc., CA, U.S.A.). All experiments were performed at room temperature (21–24°C). Numerical values were provided as the mean ± s.e.mean). Statistical analysis was performed using Student's paired two-sample *t*-test. Values of $P<0.05$ were considered significant.

External solutions and reagents

The standard external solution contained (in mM) NaCl 150, KCl 5, $CaCl_2$ 2, $MgCl_2$ 1, HEPES 10 and glucose 10. The pH was adjusted to 7.4 by adding an appropriate amount of Tris base (Sigma Chemical Co., MO, U.S.A.). For analysing the NMDA-induced current, $MgCl_2$ was removed from the standard external solution and 1 μM glycine was added. In Mg^{2+}-free external solutions, the maximal NMDA-induced inward current in rat spinal cord dorsal horn and nucleus tractus solitarii neurons is obtained in the presence of 5–10 μM glycine (Shirasaki *et al*., 1990). However, concentrations of glycine above 3 μM activates Cl^- currents in rat DMV neurons (Doi *et al*., 1999) and strychnine has been reported to elicit Ca^{2+}-dependent K^+ currents in rat dorsal ganglion cells (Aibara *et al*., 1991) and hippocampal CA1 neurons (Ebihara & Akaike, 1992). Therefore, in the present study, all recordings were performed in a Mg^{2+}-free external solution containing 1 μM glycine.

Tri-*n*-butyltin (TBT) chloride (Tokyo Kasei Co., Tokyo, Japan) was dissolved in dimethyl sulphoxide (DMSO), resulting in a 100 μM stock solution. Although the purity of TBT was 98%, the contaminants, such as di-*n*-butyltin and mono-*n*-butyltin, are less toxic than TBT (Snoeij *et al*., 1987), suggesting that they do not contribute to TBT's toxicity to a large extent. Apamine, charybdotoxin and iberiotoxin (Peptide Institute, Osaka, Japan) were dissolved in distilled water to give a 100 μM stock solution. Tolbutamide (Wako, Tokyo, Japan) was dissolved in 0.1 N NaOH, to give a 100 mM stock solution. The stock solutions were added to the external solution just before to give the desired concentrations. The final concentration of DMSO never exceeded 0.1%, which had no effect on the membrane currents. Rapid application of solution to the dissociated neurons was achieved using a 'Y-tube' perfusion system, as described previously (Murase *et al*., 1990).

Results

Effects of TBT on NMDA-induced membrane currents

As shown in Figure 1A, the application of NMDA to dissociated DMV neurons held at a potential (V_H) of −40 mV elicited an inward current which was followed by an outward current, evident immediately upon washout of NMDA. The amplitude of the inward current, and subsequent outward current, were dependent on the NMDA concentration. The half-maximum effective concentration (EC_{50}) for activation of the inward current was 21.2 μM, and the current reached its maximum amplitude at a NMDA concentration of 300 μM or more (Figure 1B).

The effect of 100 nM TBT on currents induced by 100 μM NMDA was examined at a V_H of −40 mV. TBT was applied 1 min before the first application of NMDA, since prolonged application of 100 nM TBT to isolated neurons sometimes induced an irreversible, large inward current (Kishimoto *et al*., 2001). TBT itself induced a small outward current in rat DMV neurons (note the change in holding currents in Figure 2A), slightly decreased the amplitude of the NMDA-induced inward current and, most notably, markedly increased the subsequent outward current (Figure 2).

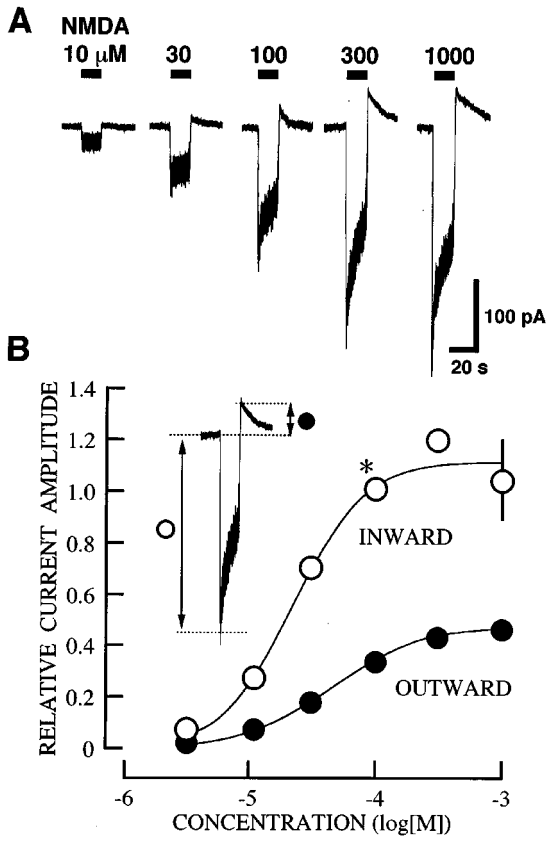

Figure 1 NMDA-induced currents in rat DMV neurons. The holding potential (V_H) was −40 mV. (A) Typical traces of currents induced by increasing concentration of NMDA. Closed bars above the current traces show the period of application of NMDA. (B) Concentration-response relationship for NMDA-induced inward (open circle) and outward currents (filled circle). The amplitude of the current induced by each NMDA concentration was normalized to the amplitude of the inward current induced by 100 μM NMDA. Symbol and error bars are mean and s.e.mean of four experiments. Error bars are sometimes obscured by the symbols.

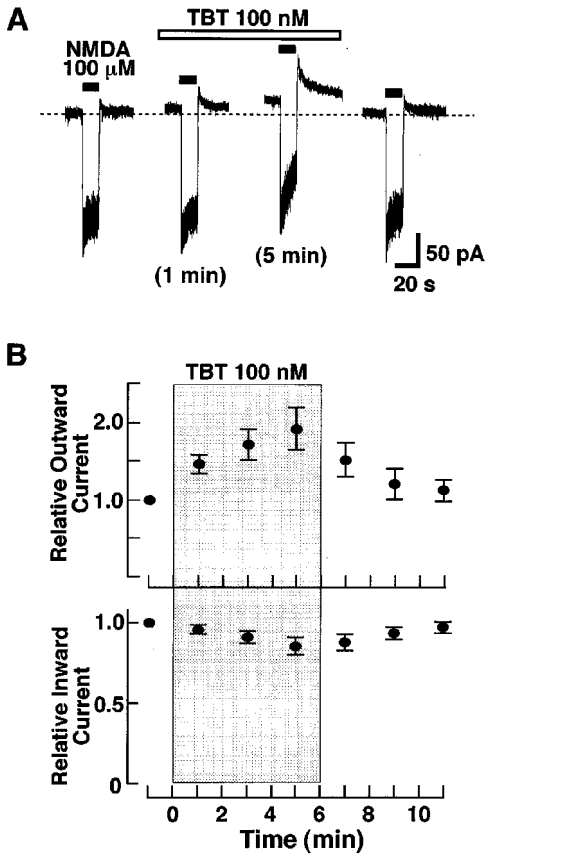

Figure 2 Effects of TBT on NMDA-induced currents. (A) NMDA-induced currents in control conditions, 1 and 5 min after the application of TBT, and after wash-out of TBT. Filled bars indicate the period of application of 100 μM NMDA. Note the outwardly shifted holding current during TBT application. (B) Time course of the changes in peak inward and outward currents during the application of TBT. NMDA (100 μM) was applied every 2 min. Symbol and error bars are the mean and s.e.mean of four experiments.

Ionic nature of the outward currents

To determine the ionic basis of the NMDA-induced outward current which was potentiated by TBT, we investigated the current-voltage ($I-V$) relationship of this current between −40 and −110 mV using voltage ramps (Murai *et al*., 1997). As shown in Figure 3A, the voltage ramp was applied both before the application of NMDA and immediately after washing out of NMDA, all in the continued presence of TBT. The reversal potential of the NMDA-induced outward current was -87.6 ± 2.9 mV ($n=4$), close to calculated K^+ equilibrium potential of −85.7 mV. We further investigated the ionic basis of this current by replacing the K^+ in the internal pipette solution with Cs^+. As shown in Figure 3B, the outward current was completely suppressed under these conditions. Both these experiments clearly demonstrates that the outward current is mediated by efflux of K^+ ions, implicating the involvement of K^+ channels. Furthermore, under these experimental conditions where the outward current was suppressed, TBT had no effect on the NMDA-induced inward current.

Identification of the outward current as Ca^{2+}-activated K^+ current

The high Ca^{2+} permeability of the NMDA channels (Meyer & Westbrook, 1987) raised the possibility that the outward K^+ current described above is a Ca^{2+}-activated K^+ current (I_{KCa}). Thus, to explore this possibility, we performed the following experiments. Firstly we investigated the NMDA-induced outward current in TBT-treated neurons in the absence of extracellular Ca^{2+}. As shown in Figure 4A, the outward current was completely suppressed under these conditions. Furthermore, the outward current was fully suppressed by 300 nM charybdotoxin (a blocker for large and intermediate conductance I_{KCa}) and 5 mM tetraethylammonium (a nonspecific blocker for I_{KCa}), but not by 1 μM apamin (a blocker for small conductance I_{KCa}), 300 nM iberiotoxin (an blocker for intermediate conductance I_{KCa}) or 300 μM tolbutamide (a blocker for ATP-sensitive K^+ current) (Figure 4B,C). These results indicate that TBT increases the amplitude of an NMDA-induced charybdotoxin-sensitive I_{KCa}.

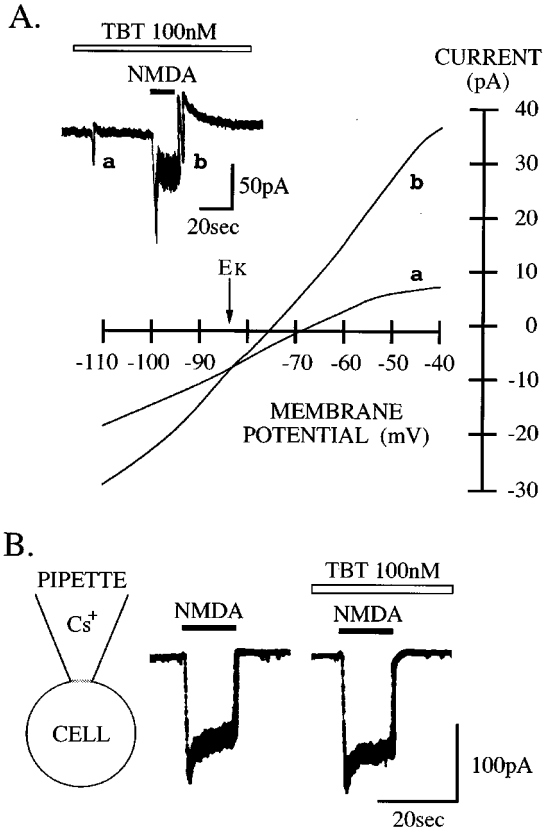

Figure 3 Contribution of K^+ channels to the outward current. (A) Current-voltage ($I-V$) relationship of NMDA-induced outward current in the presence of TBT. The holding potential was ramped from -40 to -100 mV at a rate of 45 mV s^{-1}. The current traces labelled a and b were in response to voltage ramps applied before and immediately after, the application of NMDA, as indicated in the inset. (B) Effect of TBT on the NMDA-induced inward current. The outward current carried by K^+ was completely suppressed by substitution of K^+ in the pipette solution with Cs^+. Under these conditions there is no effect of TBT on the NMDA-induced inward current. The holding potential was -40 mV. TBT was applied 1 min before the NMDA application.

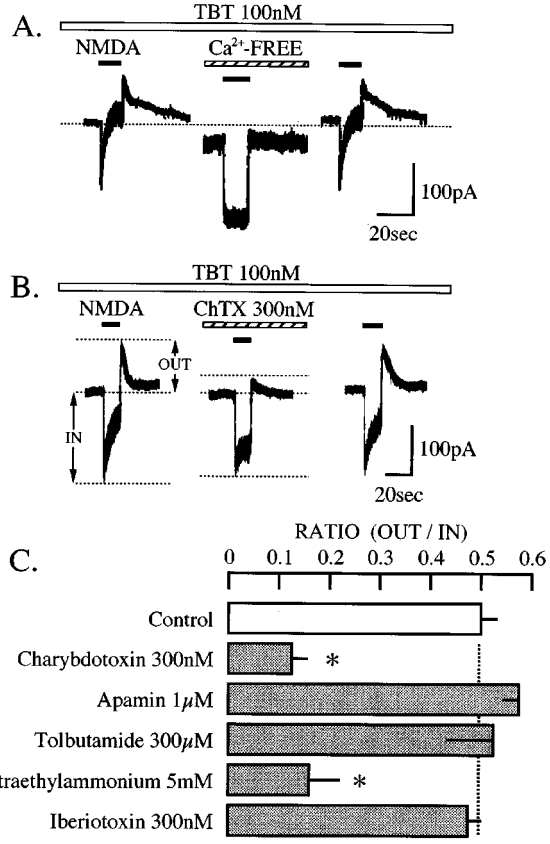

Figure 4 Pharmacological characterization of the NMDA-induced outward current, augmented by TBT. (A) NMDA-induced currents, in the absence of extracellular Ca^{2+}, in a DMV neuron pretreated with TBT. The dotted lines show the holding current before the application of TBT. (B) The effect of 300 nM charybdotoxin on the NMDA-induced currents in a neuron treated with TBT. (C) Pharmacological characterization of NMDA-induced outward current, augmented by TBT. The column height and error bars indicate the mean and s.e.mean. of four experiments. The dotted line indicates the control current amplitude in the absence of drug. Asterisks (*) indicate a significant decrease in the outward current, as compared to the control ($P<0.01$).

Discussion

TBT is a highly toxic organotin pollutant that, despite its prohibition, continues to contaminate the marine environment in Japan and other countries. It has been reported to accumulate in mollusks and fish at concentrations of, for example, 27–202 ng g^{-1} in fish muscle and 54–223 ng g^{-1} in fish liver (Shawky & Emons, 1998). Higher total concentrations of butyltin compounds including mono-, di- and tributyltin are accumulated further up the food chain in various wild animals; e.g., 115–1007 ng g^{-1} for common cormorants (Guruge *et al*., 1996), 8.5–2610 ng g^{-1} for river otters (Kannan *et al*., 1999), and 1200–2200 ng g^{-1} for dolphins (Kannan *et al*., 1996). It seems likely then, that concentrations of TBT (molecular weight = 290) accumulated in the organs of some animals will equal or exceed the concentration of TBT (100 nM) used in the present study. Although it is difficult to assess the concentration of TBT in human brains, a shopping basket survey of Japanese marketgoers resulted in an estimate for the human daily intake of TBT of 2.29 μg (Sekizawa, 1998). Thus, it is quite possible that TBT may accumulate in some human organs to the nanomolar concentrations with potential toxic actions.

TBT at the concentration of 100 nM seemed to inhibit the NMDA-induced inward current when the neurons were perfused with standard pipette solution containing 150 mM K^+, and it augmented the outward current that is clearly observed after washing-out of NMDA in rat DMV neurons (Figure 2). On the other hand, when the Cs^+ internal solution was used (Figure 3B), TBT had no effect on the NMDA-induced inward current and the NMDA-induced outward current was deleted completely. Thus, the suppression of the NMDA-induced inward current observed with the standard pipette solution might be due to the potentiating effect of TBT on the NMDA-induced outward current.

The reversal potential of NMDA-induced outward current in the presence of TBT was close to the E_K (Figure 3A), calculated with the Nernst equation and the given external and internal concentrations of K^+. The present study used the nystatin-perforated patch recording technique. Nystatin

forms small pores in the membrane under the patch pipette that allows small monovalent ions to pass, while the large anions in the cell are not expected to be permeant. This situation is essentially a Donnan equilibrium. Thus, one can predict that there will be a difference in the K^+ concentration in the pipette and in the cell, and that the junction potential across the patch membrane may also affect the measurement of reversal potential. Although the junction potential would, in some instances, hinder the accurate analysis of voltage-dependent processes, the reversal potential measurements are not affected. At the reversal potential, where there is no net flow of ions, the contribution of the intracellular concentration would be canceled and the reversal potential is determined solely from the ratio of intrapipette and extracellular concentrations (Horn & Marty, 1988).

The outward current induced by NMDA observed after withdrawal of NMDA in the presence of TBT was identified as I_{KCa} because it had a reversal potential near the theoretical K^+ equilibrium potential (Figure 3A), was blocked by internal Cs^+ and external charybdotoxin, and was dependent on Ca^{2+}-influx through the NMDA receptor channels (Figure 4). Insensitivity of the outward current to tolbutamide confirms that it is not an ATP-sensitive K^+ current.

TBT, at a concentration of 100 nM, causes a small increases in $[Ca^{2+}]_i$ in murine cerebellar neurons and thymocytes, by both increasing membrane Ca^{2+} permeability and by releasing Ca^{2+} from intracellular stores (Chikahisa & Oyama, 1992; Oyama *et al*., 1994; Ueha *et al*., 1996). In the present study, the application of TBT by itself produced an outward shift in the holding current (Figure 2), while the application of charybdotoxin to a TBT treated neuron produced an inward shift in the holding current (Figure 4). Thus, it seems that 100 nM TBT also increases $[Ca^{2+}]_i$ in rat DMV neurons resulting in the activation of I_{KCa}. Increases in cytoplasmic Ca^{2+} are normally regulated by ATP-driven sequestration into intracellular organelles and extrusion into the extracellular space, by Na^+/Ca^{2+} exchange across the cytoplasmic membrane, and by binding to intracellular Ca^{2+}-binding proteins. Dysfunction of any of these factors hampers and removal of Ca^{2+} and leads to more prolonged elevation of cytoplasmic Ca^{2+}. Since triorganotins have been reported to inhibit the cytoplasmic Ca^{2+} pump in cardiac muscle (Kodavanti *et al*., 1991), we propose that the potentiation of NMDA-induced I_{KCa} by TBT is caused by a reduced ability of the neurons to maintain appropriate cytoplasmic Ca^{2+} homeostasis.

In conclusion, TBT increases NMDA-induced outward K^+ currents in rat brain neurons. The physiological consequences of this would be to attenuate the excitatory effect of NMDA. Since activation of NMDA receptors is linked to a variety of physiological and pathological roles in the mammalian brains (Blandini *et al*., 1996; Kaczmarek *et al*., 1997; Fedele & Raiteri, 1999; Kornhuber & Wiltfang, 1999), the attenuation of the NMDA response by TBT may have important implications for neuronal function.

The authors thank Dr A. Moorhouse for critical reading on this manuscript and correcting English. This study was supported by Grant-in-Aids from the Sumitomo Foundation (Osaka, Japan) to N. Akaike.

References

AIBARA, K., OOMURA, M. & AKAIKE, N. (1991). Strychnine-induced potassium current in isolated dorsal root ganglion cells of the rat. *Br. J. Pharmacol.,* **102,** 492–496.

AKAIKE, N. & HARATA, N. (1994). Nystatin perforated patch recording and its application to analyses of intracellular mechanisms. *Jpn. J. Physiol.,* **44,** 433–473.

BALASUBRAMANIAN, S., LYNCH, J.W. & BARRY, P.H. (1996). Calcium-dependent modulation of the agonist affinity of the mammalian olfactory cyclic nucleotidegated channel by calmodulin and a novel endogenous factor. *J. Membr. Biol.,* **152,** 13–23.

BLANDINI, F., PORTER, R.H. & GREEAMYRE, J.T. (1996). Glutamate and Parkinson's disease. *Mol. Neurobiol.,* **12,** 73–94.

CHIKAHISA, L. & OYAMA, Y. (1992). Tri-*n*-butyltin increases intracellular Ca^{2+} in mouse thymocytes: a flow cytometric study using fluorescent dyes for membrane potential and intracellular Ca^{2+}. *Pharmacol. Toxicol.,* **71,** 190–195.

DE-KONINCK, Y. & MODY, I. (1996). The effects of raising intracellular calcium on synaptic GABAA receptor-channels. *Neuropharmacol.,* **35,** 1365–1374.

DOI, A., KISHIMOTO, K. & ISHIBASHI, H. (1999). Modulation of glycine-induced currents by zinc and other metal cations in neurons acutely dissociated from the dorsal motor nucleus of the vagus of the rat. *Brain Res.,* **816,** 424–430.

EBIHARA, S. & AKAIKE, N. (1992). Strychnine-induced potassium current in CA1 pyramidal neurones of the rat hippocampus. *Br. J. Pharmacol.,* **106,** 823–827.

EMA, M., ITAMI, T. & KAWASAKI, H. (1991a). Behavioral effects of acute exposure to tributyltin chloride in rats. *Neurotoxicol. Teratol.,* **13,** 489–493.

EMA, M., ITAMI, T. & KAWASAKI, H. (1991b). Changes of spontaneous motor activity of rats after acute exposure to tributyltin chloride. *Drug. Chem. Toxicol.,* **14,** 161–171.

FEDELE, E. & RAITERI, M. (1999). In vivo studies of the cerebral glutamate receptor/NO/cGMP pathway. *Prog. Neurobiol.,* **58,** 89–120.

GHONEUM, M., HUSSEIN, A.E., GILL, G. & ALFRED, L.J. (1990). Suppression of murine natural killer cell activity by tributyltin: in vivo and in vitro assessment. *Environ. Res.,* **52,** 178–186.

GURUGE, K.S., TANABE, S., IWATA, H., TATSUKAWA, R. & YAMAGISHI, S. (1996). Distribution, biomagnification, and elimination of butyltin compound residues in common cormorant (*Phalacrorax carbo*) from Lake Biwa, Japan. *Arch. Environ. Contam. Toxicol.,* **31,** 210–217.

HARINO, H., FUKUSHIMA, M. & KAWAI, S. (2000). Accumulation of butyltin and phenyltin compounds in various fish species. *Arch. Environ. Contam. Toxicol.,* **39,** 13–19.

HORN, R. & MARTY, A. (1988). Muscarinic activation of ionic currents measured by a new whole-cell recording method. *J. Gen. Physiol.,* **92,** 145–159.

INOUE, M., OOMURA, Y., YAKUSHIJI, T. & AKAIKE, N. (1986). Intracellular calcium ions decrease the affinity of the GABA receptor. *Nature,* **324,** 156–158.

KACZMAREK, L., KSOOUT, M. & SKANGIEL-KRAMSKA, J. (1997). Glutamate receptors in cortical plasticity: molecular and cellular biology. *Physiol. Rev.,* **77,** 217–255.

KANNAN, K., CORSOLINI, S., FORCARDI, S., TANABE, S. & TATSUKAWA, R. (1996). Accumulation pattern of butyltin compounds in dolphin, tuna and shark collected from Italian coastal waters. *Arch. Environ. Contam. Toxicol.,* **31,** 19–23.

KANNAN, K., GRIVE, R.A., SENTHILKUMAR, K., HENNY, C.J. & GIESY, J.P. (1999). Butyltin compounds in river otters (*Lutra canadensis*) from the northwestern United States. *Arch. Environ. Contam. Toxicol.,* **36,** 462–468.

KISHIMOTO, K., MATSUO, S., KANEMOTO, Y., ISHIBASHI, H., OYAMA, Y. & AKAIKE, N. (2001). Nanomolar concentrations of tri-n-butyltin facilitate γ-aminobutyric acidergic synaptic transmission in rat hypothalamic neurons. *J. Pharmacol. Exp. Ther.,* **299,** 171 – 177.

KORNHUBER, J. & WILTFANG, J. (1999). The role of glutamate in dementia. *J. Neural Transm.,* **53** (Suppl.): 277 – 287.

KODAVANTI, P.R., CAMERON, J.A., YALLAPRAGADA, P.R., VIG, P.J. & DESAIAH, D. (1991). Inhibition of Ca^{2+} transport associated cAMP-dependent protein phosphorylation in rat cardiac sarcoplasmic reticulum by triorganotins. *Arch. Toxicol.,* **65,** 311 – 317.

KYROZIS, A., ALBUQUERQUE, C., GU, J. & MACDERMOTT, A.B. (1996). Ca^{2+}-dependent inactivation of NMDA receptors: fast kinetics and high Ca^{2+} sensitivity in rat dorsal horn neurons. *J. Physiol. Lond.,* **495,** 449 – 463.

LUIJTEN, J.G. (1971). Application and biological effects of organotin compounds. In *Organotin Compounds,* ed. Sawyer AK pp. 931 – 974, New York: Decker.

MEYER, M.L. & WESTBROOK, G.L. (1987). Permeation and block of N-methyl-D-aspartic acid receptor channels by divalent cations in mouse cultured central neurons. *J. Physiol. (Lond.),* **394,** 501 – 527.

MURAI, Y., ISHIBASHI, H., KOYAMA, S. & AKAIKE, N. (1997). Ca^{2+}-activated K^+ currents in rat locus coeruleus neurons induced by experimental ischemia, anoxia and hypoglycemia. *J. Neurophysiol.,* **78,** 2674 – 2681.

MURASE, K., RANDIC, M., SHIRASAKI, T., NAKAGAWA, T. & AKAIKE, N. (1990). Serotonin suppresses N-methyl-D-aspartate responses in acutely isolated spinal dorsal horn neurons of the rat. *Brain Res.,* **525,** 84 – 91.

O'CALLAGHAN, J.P. & MILLER, D.B. (1988). Acute exposure of the neonatal rat to butyltin results in decreases in biochemical indicators of synaptogenesis and myelinogenesis. *J. Pharmacol. Exp. Ther.,* **246,** 394 – 402.

OHHIRA, S., MATSUI, H. & WATANABE, K. (1999). Effects of pretreatment with cytochrome P-450 inducers, especially phenobarbital on triphenyltin metabolism and toxicity in hamsters. *Toxicology,* **137,** 151 – 159.

OYAMA, Y., UEHA, T. & HAYASHI, A. (1993). Effect of tri-*n*-butyltin on intracellular Ca^{2+} concentration of rat cerebellar neurons. *Eur. J. Pharmacol.,* **248,** 89 – 93.

OYAMA, Y., UEHA, T., HAYASHI, A. & CHIKAHISA, L. (1994). Effects of tri-*n*-butyltin on intracellular Ca^{2+} concentration of mouse thymocytes under Ca^{2+}-free condition. *Eur. J. Pharmacol.,* **270,** 137 – 142.

RAFFRAY, M. & COHEN, G.M. (1993). Thymocyte apoptosis as a mechanism for tributyltin-induced thymic atrophy in vivo. *Arch. Toxicol.,* **67,** 231 – 236.

SEKIZAWA, J. (1998). Health and environmental risk assessment of organotin pollution in Japan (in Japanese). *Kokuritsu Iyakushin Shokuhin Eisei Kenkyusho Houkoku,* **116,** 126 – 131.

SHAWKY, S. & EMONS, H. (1998). Distribution pattern of organotin compounds at different trophic levels of aquatic ecosystems. *Chemosphere,* **36,** 523 – 535.

SHIM, W.J., OH, J.R., KAHNG, S.H., SHIM, J.H. & LCE, S.H. (1998). Accumulation of tributyl- and triphenyltin compounds in Pacific oyster, *Crassostrea gigas*, from the Chinhac Bay System, Korea. *Arch. Environ. Contamin. Toxicol.,* **35,** 41 – 47.

SHIRASAKI, T., NAKAGAWA, T., WAKAMORI, M., TATEISHI, N., FUKUDA, A., MURASE, K. & AKAIKE, N. (1990). Glycine-insensitive desensitization of N-methyl-D-aspartate receptors in acutely isolated mammalian central neurons. *Neurosci. Lett.,* **108,** 93 – 98.

SNOEIJ, N.J., PENNINKS, A.H. & SEINEN, W. (1987). Biological activity of organotin compounds - an overview. *Environ. Res.,* **44,** 335 – 353.

UEHA, T., OYAMA, Y. & TOMIYOSHI, F. (1996). Cytotoxic action of tri-*n*-butyltin on dissociated cerebellar neurones: a flow-cytometric study. *Pharmacol. Toxicol.,* **78,** 404 – 408.

WHALEN, M.M., LOGANATHAN, B.G. & KANNAN, K. (1999). Immunotoxicity of environmentally relevant concentrations of butyltins on human natural killer cells in vitro. *Environ. Res.,* **81,** 108 – 116.

YAMAMOTO, I. (1994). Pollution of fish and shellfish with organotin compounds and estimation of daily intake (in Japanese). *Hokkaido Igaku Zasshi,* **69,** 273 – 281.

(Received October 31, 2001
Revised February 26, 2002
Accepted February 28, 2002)